

# Absorption Spectrum of Singlet Oxygen ( $a^1\Delta_g \rightarrow b^1\Sigma_g^+$ ) in $D_2O$ : Enabling the Test of a Model for the Effect of Solvent on Oxygen's Radiative Transitions

Lars Klemmt Andersen and Peter R. Ogilby\*

Department of Chemistry, University of Aarhus, Langelandsgade 140, DK-8000 Århus, Denmark

Received: June 21, 2002

The time-resolved absorption spectrum of singlet molecular oxygen ( $a^1\Delta_g \rightarrow b^1\Sigma_g^+$ ) has been recorded in liquid  $D_2O$  using a step-scan Fourier transform spectrometer. A molar absorption coefficient of  $6 \pm 2 \text{ M}^{-1} \text{ cm}^{-1}$  was determined for the peak of the absorption band at  $5228 \pm 6 \text{ cm}^{-1}$ . In this report, issues pertinent to the detection of this signal are outlined. Specifically, for  $O_2(a^1\Delta_g)$  produced upon pulsed laser irradiation of a sensitizer, it is necessary to account for a laser-induced, temperature-dependent shift in a  $D_2O$  absorption band that interferes with the weak  $a \rightarrow b$  signal. Along with  $a \rightarrow b$  absorption coefficients obtained previously in other solvents, the  $D_2O$  data reported herein enable an appropriate test of a topical model for the perturbing effect of solvent on radiative transitions in oxygen.

## Introduction

The lowest excited electronic state of molecular oxygen,  $O_2(a^1\Delta_g)$ , routinely called singlet oxygen, is important to a range of disciplines, in part, because of its unique reactivity.<sup>1</sup> For example,  $O_2(a^1\Delta_g)$  is a significant intermediate in the photoinduced degradation of polymers<sup>2</sup> and in photodynamic therapies for cancer treatment.<sup>3</sup> Moreover, for oxygen dissolved in a given solvent, “forbidden” transitions between  $O_2(a^1\Delta_g)$  and oxygen's ground state,  $O_2(X^3\Sigma_g^-)$ , as well as the second excited state,  $O_2(b^1\Sigma_g^+)$ , provide a system to examine mechanisms by which solvent can perturb a solute.<sup>4</sup> Therefore, the development of direct, time-resolved spectroscopic probes for  $O_2(a^1\Delta_g)$  as well as  $O_2(b^1\Sigma_g^+)$  can have important ramifications.

It is well established that  $O_2(a^1\Delta_g)$  can be monitored by its  $a \rightarrow X$  phosphorescence at  $\sim 7850 \text{ cm}^{-1}$  in many solvents and that  $O_2(b^1\Sigma_g^+)$  can be monitored by its  $b \rightarrow a$  fluorescence at  $\sim 5200 \text{ cm}^{-1}$  in some solvents.<sup>5,6</sup> Of course, luminescence measurements offer many advantages in the detection of weak transitions, and a great deal of information has been obtained with these spectroscopic tools.<sup>5–8</sup> We recently demonstrated a complementary technique by which  $O_2(a^1\Delta_g)$  can be probed, showing that the  $a \rightarrow b$  transition can be monitored in a time-resolved absorption experiment at  $\sim 5200 \text{ cm}^{-1}$ .<sup>9</sup> Despite the classic limitation that weak transitions are generally difficult to monitor in an absorption experiment, we have established that the approach nevertheless provides unique and useful data in a variety of organic solvents.<sup>10–12</sup>

It is now acknowledged that the rate constant for the  $a \rightarrow X$  radiative transition,  $k_{aX}$ , depends significantly on the solvent.<sup>13–15</sup> For example,  $k_{aX}$  in  $CS_2$  is  $\sim 17$  times larger than  $k_{aX}$  in  $D_2O$ . At present, the most promising model that accounts for this effect of solvent on  $k_{aX}$  is that of Minaev.<sup>16–18</sup> The principal tenet of Minaev's thesis is that the  $a \rightarrow X$  transition borrows intensity from the  $b \rightarrow a$  transition by virtue of a spin-orbit interaction that mixes the  $O_2(b^1\Sigma_g^+)$  and  $O_2(X^3\Sigma_g^-)$  states. Any solvent-dependent change in the probability of the  $b \rightarrow a$  transition will thus be manifested in the  $a \rightarrow X$  transition. The  $b \rightarrow a$  transition is proposed to gain intensity via a solvent-

dependent disruption of oxygen's cylindrical symmetry that, in turn, lifts the degeneracy of oxygen's  $\pi_x$  and  $\pi_y$  antibonding orbitals. In making a solvent-dependent distinction between the  $\pi_x$  and  $\pi_y$  orbitals, a solvent-dependent dipolar component is introduced into the  $b \rightarrow a$  transition. In comparison with the unperturbed  $b \rightarrow a$  transition, which is allowed only as an electric quadrupole process, the solvent-induced electric dipole character causes a significant increase in the  $b \rightarrow a$  transition probability.

This thesis, that solvent-dependent changes in the probability of the  $a \rightarrow X$  transition derive from solvent-dependent changes in the probability of the  $b \rightarrow a$  transition, has an interesting consequence. In Minaev's model, the ratio  $k_{aX}/k_{ba}$  is predicted to be solvent-independent with a value of  $\sim 3 \times 10^{-4}$ .<sup>18</sup>

Recently, significant support for Minaev's model has come from Schmidt and co-workers.<sup>19,20</sup> Unfortunately, however, experimental limitations preclude a study of the  $b \rightarrow a$  transition in a wide range of solvents; the  $O_2(b^1\Sigma_g^+)$  lifetime is simply too short in solvents that contain C–H, C–D, O–H, or O–D bonds to enable detection using currently available tools.<sup>21</sup> Thus, it has been necessary to rely on gas-phase  $b \rightarrow a$  data in the application of Minaev's model to the interpretation of solution-phase  $a \rightarrow X$  data.<sup>19,20</sup> Although such a comparison has its positive aspects (i.e., it potentially shows the “universality” of the model), it would nevertheless be desirable to first show the viability of Minaev's thesis using  $b \rightarrow a$  data from liquid solvents. To this end, rather than using  $b \rightarrow a$  emission data, the complementary  $a \rightarrow b$  absorption data can be useful, particularly if  $a \rightarrow b$  spectra can be recorded from a range of solvents that include water, some hydrocarbons, and molecules that lack C–H and O–H bonds (e.g.,  $CS_2$ ).

Water is one of the more important solvents for which a spectroscopic probe of  $O_2(a^1\Delta_g)$  can provide useful information. Studies in water are not only significant with respect to biological processes, but the specific solvation effects of water provide important insight when examining methods by which solutes, such as oxygen, can be perturbed. For the present study, we set out to ascertain if  $O_2(a^1\Delta_g)$  could be detected via the  $a \rightarrow b$  transition in an aqueous system.

The spectroscopic detection of  $O_2(a^1\Delta_g)$  can be difficult in aqueous systems due, in part, to the low solubility of oxygen

\* To whom correspondence should be addressed.

in water<sup>22</sup> and, in H<sub>2</sub>O, a comparatively short O<sub>2</sub>(a<sup>1</sup>Δ<sub>g</sub>) lifetime of ~4 μs.<sup>8,23</sup> Moreover, like the a → X transition, the a → b transition in aqueous media will most likely have a transition probability that is much smaller than in organic solvents.<sup>6,14</sup>

We now report that the time-resolved a → b absorption spectrum of O<sub>2</sub>(a<sup>1</sup>Δ<sub>g</sub>) can indeed be recorded upon the irradiation of a sensitizer in D<sub>2</sub>O. Although this work required that we address a number of issues,<sup>24</sup> it was primarily necessary to account for a transient laser-induced, temperature-dependent shift in a solvent absorption band that interfered with the desired data. The a → b data thus obtained in D<sub>2</sub>O, along with a → b data we have obtained in other solvents,<sup>9,24</sup> enable an appropriate test of Minaev's model using liquid solvents that have a large range of *k*<sub>aX</sub> and *k*<sub>ba</sub> values.

## Experimental Section

In this study, O<sub>2</sub>(a<sup>1</sup>Δ<sub>g</sub>) was produced upon 355 nm pulsed-laser irradiation of the sensitizer 1*H*-phenalen-1-one-2-sulfonic acid (perinaphthenone sulfonic acid, PNS). (From independent a → X experiments, it is known that O<sub>2</sub>(a<sup>1</sup>Δ<sub>g</sub>) is efficiently produced upon PNS irradiation.<sup>25</sup>) Using a modified Bruker IFS 66v/S step-scan Fourier transform spectrometer equipped with a 77 K InSb detector, O<sub>2</sub>(a<sup>1</sup>Δ<sub>g</sub>) was then monitored in a time-resolved absorption experiment. For these experiments, the 10–90% response time of the instrument was 280 ns. Additional details of our approach and the pertinent instrumentation appear elsewhere.<sup>10,11,24</sup>

PNS was synthesized using the method of Nonell et al.<sup>25</sup> This molecule degraded upon prolonged laser irradiation, and we thus used a flow cell to maintain a consistent sample. In this cell, the rate of sample exchange in the volume probed was much slower than the rates of the laser-induced phenomena being measured, including solvent thermal relaxation. The PNS concentration was adjusted such that the absorbance at 355 nm was ~0.5. Potassium chromate (K<sub>2</sub>CrO<sub>4</sub>, 99.5%, Merck), used as the so-called “heat-dump” (see text), was stable upon laser irradiation. D<sub>2</sub>O (99.9% D, Deutero) was used as received. For all experiments, oxygen saturated solutions were used at 1 atm in 1 mm path length quartz cuvettes.

## Results and Discussion

**Advantages of Using D<sub>2</sub>O, not H<sub>2</sub>O.** The most apparent potential limitation to the detection of the a → b absorption at ~5200 cm<sup>-1</sup> in aqueous systems is that H<sub>2</sub>O has a strong absorption band in this region.<sup>24,26</sup> The latter is due to a combination of stretching and deformation modes whose fundamental transitions occur at ~3400 and ~1640 cm<sup>-1</sup>, respectively.<sup>27</sup> D<sub>2</sub>O likewise has an absorption band at ~5200 cm<sup>-1</sup> (Figure 1a), in this case due to the first overtone (0 → 2) of the OD stretching mode. Most importantly, however, this latter band is less pronounced than the H<sub>2</sub>O band at ~5200 cm<sup>-1</sup>, at least to the extent that an attempt to detect the a → b transition at ~5200 cm<sup>-1</sup> in D<sub>2</sub>O is worthwhile. Another advantage of using D<sub>2</sub>O is that the lifetime of O<sub>2</sub>(a<sup>1</sup>Δ<sub>g</sub>) in the deuterated solvent is ~17 times longer than that in H<sub>2</sub>O.<sup>28</sup> Thus, in D<sub>2</sub>O, one can temporally discriminate between the longer-lived a → b signal and any short-lived absorption from the triplet state sensitizer.<sup>24</sup>

**Interfering Signal.** Upon 355 nm pulsed-laser irradiation of PNS in D<sub>2</sub>O, a small transient signal is observed in the range 4500–5500 cm<sup>-1</sup> that has both positive and negative absorbance changes (Figure 1b). Upon comparison of these data with the absorption spectrum of D<sub>2</sub>O (Figure 1a), it appears likely that this profile of positive and negative absorbance change could

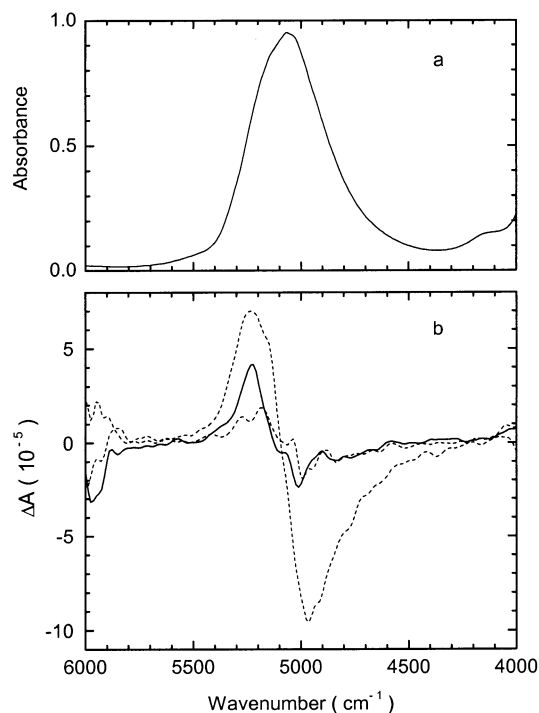


**Figure 1.** (a) Absorption spectrum of D<sub>2</sub>O recorded over the range 4000–6000 cm<sup>-1</sup> using a 1 mm path length cell. (b) Transient signal recorded upon 355 nm pulsed laser irradiation of PNS in D<sub>2</sub>O at 3.45 mJ pulse<sup>-1</sup> cm<sup>-2</sup> (solid line). Also shown are transient signals obtained upon 355 nm irradiation of K<sub>2</sub>CrO<sub>4</sub> in D<sub>2</sub>O at 3.45 and 16.8 mJ pulse<sup>-1</sup> cm<sup>-2</sup> (dashed lines). The PNS and K<sub>2</sub>CrO<sub>4</sub> data were collected over the period 4–14 μs after the laser pulse using optically matched solutions (*A* = 0.5 at 355 nm).

be a consequence of a laser-dependent shift in the D<sub>2</sub>O absorption band. Therefore, we set out to independently investigate this possibility.

It is known from steady-state experiments that the position of the IR absorption bands in H<sub>2</sub>O depends on the sample temperature; the bands shift to a larger wavenumber with a temperature increase.<sup>29,30</sup> This effect derives from temperature-dependent changes in the extent of hydrogen bonding in the system. It has also recently been shown that a laser-induced temperature increase causes a shift to larger wavenumbers in the ~3400 cm<sup>-1</sup> band of H<sub>2</sub>O.<sup>31</sup> In turn, this shift yields a transient signal similar to that shown in Figure 1b for D<sub>2</sub>O.

To better characterize such thermal effects, it is desirable to have a mechanism by which heat can be deposited into the system in a rapid and controlled fashion. To this end, K<sub>2</sub>CrO<sub>4</sub> was used as a so-called “heat-dump”. Upon irradiation with a pulsed laser, the light energy absorbed by this molecule is rapidly lost (<1 μs) to the surrounding medium in a nonradiative process.<sup>24,32</sup> Indeed, upon 355 nm pulsed laser irradiation of K<sub>2</sub>CrO<sub>4</sub> dissolved in D<sub>2</sub>O, the D<sub>2</sub>O absorption band at ~5050 cm<sup>-1</sup> clearly shifts to a higher wavenumber. This is manifested in the transient absorption spectrum as a feature that has both positive and negative absorbance changes (Figure 1b). Although the time scale with which this shift of the solvent band occurs is very rapid (i.e., it is concurrent with the rapid deposition of heat from K<sub>2</sub>CrO<sub>4</sub>), relaxation to the original equilibrium position occurs on the millisecond time scale.<sup>24</sup>

Upon pulsed laser irradiation of a typical singlet oxygen sensitizer, essentially all of the energy absorbed is eventually deposited as heat to the surrounding medium.<sup>33</sup> A significant portion of the total energy is deposited rapidly (<1 μs) as a consequence of photophysical events that precede or are

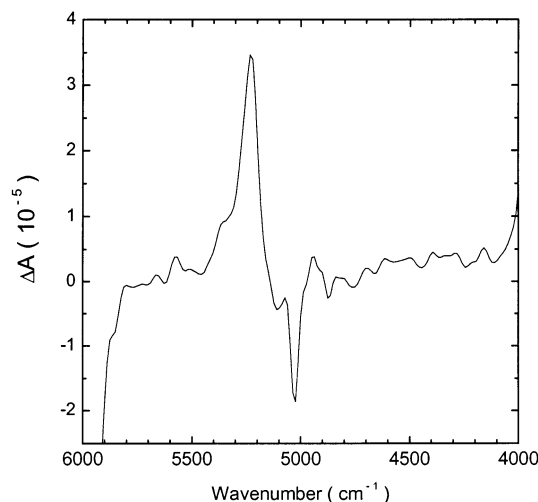


**Figure 2.** Transient absorption spectrum obtained upon subtracting the  $\text{K}_2\text{CrO}_4$ -derived signal from the PNS-derived signal for experiments in  $\text{D}_2\text{O}$ . The band with a maximum at  $5228 \pm 6 \text{ cm}^{-1}$  can be assigned to the  $a \rightarrow b$  transition of singlet oxygen.

associated with singlet oxygen production (e.g., internal conversion, intersystem crossing). Once  $\text{O}_2(a^1\Delta_g)$  is formed, however, its excitation energy of 94 kJ/mol will be lost as heat on a much longer time scale, the duration of which depends on the singlet oxygen lifetime. Thus, irradiation of PNS in  $\text{D}_2\text{O}$  is indeed expected to yield a transient signal similar to that observed upon irradiation of  $\text{K}_2\text{CrO}_4$  in  $\text{D}_2\text{O}$ .

**The  $a \rightarrow b$  Signal in  $\text{D}_2\text{O}$ .** Inspection of the data recorded upon pulsed-laser irradiation of our samples reveals that the PNS-derived transient is not as symmetrically disposed as is the  $\text{K}_2\text{CrO}_4$ -derived transient (Figure 1b). This suggests that, in the PNS data, an additional signal is superposed on the signal that arises from the temperature-dependent band shift in the solvent. Because the latter is so long-lived and can essentially be treated as a baseline shift,<sup>24</sup> it is reasonable to subtract this solvent signal to isolate other signals that may be present in the PNS data.

Indeed, upon subtracting the  $\text{K}_2\text{CrO}_4$ -derived signal from the PNS-derived signal, normalized for the amount of incident energy that is deposited as rapid heat to the medium, we obtain a difference spectrum with a band centered at  $5228 \pm 6 \text{ cm}^{-1}$  (Figure 2). On the basis of previous work in which we examine how the maxima of  $a \rightarrow b$  spectra correlate with solvent parameters,<sup>12</sup> the  $a \rightarrow b$  band in  $\text{D}_2\text{O}$  is indeed expected to have a peak maximum in this region. Of course, this point alone is not sufficient to assign this band to the  $a \rightarrow b$  transition.

The  $5228 \text{ cm}^{-1}$  band shown in Figure 2 can be assigned to singlet oxygen on the basis of its kinetics. In Figure 3, we show the time evolution of the signals created upon the irradiation of both  $\text{K}_2\text{CrO}_4$  and PNS, integrated over the spectral range 4000–6000  $\text{cm}^{-1}$ . For the  $\text{K}_2\text{CrO}_4$ -derived signal, a flat baseline is obtained, reflecting the symmetry of the positive and negative absorbance changes in this spectral range. However, for the PNS-derived signal, one clearly sees distinctive changes in time. Specifically, we observe an initial rapid change in absorbance that can be assigned to the PNS triplet,<sup>24</sup> followed by a more slowly decaying signal with a lifetime expected for that of  $\text{O}_2(a^1\Delta_g)$  in  $\text{D}_2\text{O}$  of  $65 \pm 7 \mu\text{s}$  (the same lifetime was also obtained in an independent  $a \rightarrow X$  experiment using the identical  $\text{D}_2\text{O}$  solution of PNS). Moreover, by monitoring the time evolution of the PNS-derived signal over the limited spectral range 5190–5285  $\text{cm}^{-1}$ , we ascertained that the band at 5228  $\text{cm}^{-1}$  is indeed the source of the transient with a 65  $\mu\text{s}$  lifetime.

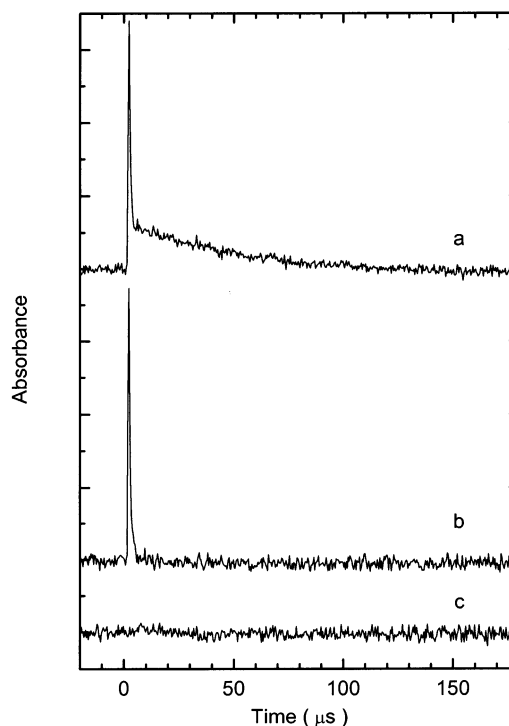


**Figure 3.** Time evolution of the signals created upon the pulsed laser irradiation of both PNS and  $\text{K}_2\text{CrO}_4$  in  $\text{D}_2\text{O}$ , integrated over the spectral range 4000–6000  $\text{cm}^{-1}$ . (a) PNS-derived signal. (b) PNS-derived signal with added  $\text{NaN}_3$ . (c)  $\text{K}_2\text{CrO}_4$ -derived signal. In each case, data from 7500 separate laser pulses were averaged.

Finally, and most conclusively, upon the addition of a  $\text{O}_2(a^1\Delta_g)$  quencher, sodium azide, the signal assigned to the  $a \rightarrow b$  transition disappears (Figure 3b).

In Figure 2, the absorbance change of  $\sim 3.5 \times 10^{-5}$  at 5228  $\text{cm}^{-1}$  corresponds to a molar absorption coefficient for the  $a \rightarrow b$  transition of  $6 \pm 2 \text{ M}^{-1} \text{ cm}^{-1}$ . This number was calculated using a quantum yield of  $\text{O}_2(a^1\Delta_g)$  production by PNS of 1.0 in  $\text{D}_2\text{O}$ <sup>25,34</sup> that, in turn, under our conditions, corresponds to a transient  $\text{O}_2(a^1\Delta_g)$  concentration of  $\sim 5.8 \times 10^{-5} \text{ M}$  that is being probed over the 1 mm path length.

**Effect of Solvent on Oxygen's Radiative Transitions: Testing the Models.** Data obtained from the  $a \rightarrow b$  absorption experiment in  $\text{D}_2\text{O}$  are listed in Table 1 along with corresponding data we have obtained from analogous  $a \rightarrow b$  experiments in other solvents. It is clear from the data shown that there is a pronounced solvent effect on the peak position of the  $a \rightarrow b$  absorption band ( $\nu_{\text{max}}$ ), on the full-width of the absorption band at half-maximum ( $\Delta\nu_{\text{fwhm}}$ ), and on the absorption coefficient at the band maximum ( $\epsilon_{\text{max}}$ ).

To facilitate data analysis within the context of Minaev's model, it is necessary to obtain rate constants,  $k_{\text{ba}}$ , for the  $b \rightarrow a$  radiative transition from the  $a \rightarrow b$  data shown in Table 1. (Note that the first-order rate constant  $k_{\text{ba}}$  is the Einstein coefficient  $A$  for spontaneous  $\text{O}_2(b^1\Sigma_g^+)$  emission.) To this end, an expression provided by Strickler and Berg<sup>35</sup> can be used (eq 1). For a transition between an upper and lower state,  $k_{\text{emission}}$

$$k_{\text{emission}} = n^2 \frac{8\pi c \ln(10) g_{\text{lower}} \nu^2 \Gamma}{N_A g_{\text{upper}}} \quad (1)$$

is the first-order radiative rate constant with the units of  $\text{s}^{-1}$ ,  $\Gamma$  is the integrated absorption coefficient in  $\text{M}^{-1} \text{ cm}^{-2}$ ,  $\nu$  is the transition frequency in  $\text{cm}^{-1}$ ,  $N_A$  Avogadro's number, and  $c$  is the speed of light. The ratio  $g_{\text{lower}}/g_{\text{upper}}$  accounts for differences

**TABLE 1: Solvent Parameters and Data Obtained from a → b Absorption Experiments**

solvent	$n^2$	$R$ (mL mol <sup>-1</sup> )	[solv] (mol L <sup>-1</sup> )	$\nu_{\max}(a \rightarrow b)$ (cm <sup>-1</sup> )	$\Delta\nu_{\text{fwhm}}$ (cm <sup>-1</sup> )	$\epsilon_{\max}(a \rightarrow b)$ (M <sup>-1</sup> cm <sup>-1</sup> )
D <sub>2</sub> O	1.790	3.77	55.3	5228	75 <sup>a</sup>	6 ± 2
CS <sub>2</sub>	2.647	21.5	16.5	5168 <sup>b</sup>	90 <sup>b</sup>	52 ± 5 <sup>c</sup>
benzene	2.253	26.3	11.2	5197 <sup>b</sup>	76 <sup>b</sup>	56 ± 6 <sup>d</sup>
<i>n</i> -hexane	1.891	29.9	7.65	5199 <sup>b</sup>	69 <sup>b</sup>	40 ± 4 <sup>c</sup>
toluene	2.238	31.1	9.40	5191 <sup>b</sup>	74 <sup>b</sup>	56 ± 6 <sup>c</sup>

<sup>a</sup> Estimated from correlation between a → b and a → X bandwidths<sup>12</sup> with an error of ±4 cm<sup>-1</sup> (see text). <sup>b</sup> From Dam et al.<sup>12</sup> Error of ±1 cm<sup>-1</sup> on  $\nu_{\max}$  and ±2 cm<sup>-1</sup> on  $\Delta\nu_{\text{fwhm}}$ . <sup>c</sup> From Weldon and Ogilby.<sup>9</sup> Values originally reported have been rounded-off and errors have been noted. <sup>d</sup> From Andersen and Ogilby.<sup>24</sup>

**TABLE 2: Radiative Rate Constants for Both the a → X and b → a Transitions**

solvent	$R$ (mL mol <sup>-1</sup> )	$k_{aX}^a$ (s <sup>-1</sup> )	$k_{ba}^b$ (s <sup>-1</sup> )	$k_{ba}^b$ (s <sup>-1</sup> M <sup>-1</sup> )	$k_{aX}/k_{ba}$ (10 <sup>-4</sup> )	$k_{ba}(\text{norm})^c$
D <sub>2</sub> O	3.77	0.18	200 ± 68	3.6 ± 1.2	9.0 ± 3.1	1.6 ± 0.5
CS <sub>2</sub>	21.5	3.1	3000 ± 330	182 ± 20	10.5 ± 1.3	104 ± 11
benzene	26.3	1.5	2346 ± 258	210 ± 23	6.5 ± 0.8	158 ± 17
<i>n</i> -hexane	29.9	0.6	1278 ± 141	168 ± 18	4.7 ± 0.6	166 ± 18
toluene	31.1	1.44	2264 ± 250	240 ± 26	6.5 ± 0.8	196 ± 22

<sup>a</sup> From Poulsen et al.,<sup>39</sup> and references therein. Errors on values of  $k_{aX}$  relative to a standard value in benzene are small (∼±5%). However, the error on the absolute value of  $k_{aX}$  in benzene is large (∼±30%).<sup>15</sup> <sup>b</sup> Calculated from a → b absorption data using the Strickler–Berg expression (see text). For the solvents toluene, *n*-hexane, and CS<sub>2</sub>, differences between the  $k_{ba}$  data reported here and values reported earlier<sup>9</sup> reflect the increased accuracy with which  $\Gamma$  can now be determined.<sup>12</sup> <sup>c</sup> Relative value of the second-order rate constant for the b → a radiative transition normalized according to the method of Hild and Schmidt<sup>20</sup> for the size of the perturbing solvent molecule and the collision frequency (see text).

in the degeneracies of the respective states and, because the a<sup>1</sup>Δ<sub>g</sub> state is doubly degenerate, has a value of 2 for the b → a transition. Moreover, because the Stokes shift between the a → b and b → a transitions is extremely small,<sup>11</sup> it is sufficient to simply use values of  $\nu_{\max}$  given in Table 1 for the transition frequency  $\nu$ . It is important to note, however, that eq 1 was developed for allowed transitions and, for the nominally forbidden a → b transition in oxygen, may not yield accurate values of the rate constant  $k_{ba}$ .<sup>6,36</sup> Nevertheless, as a means to represent relative, solvent-dependent changes in  $k_{ba}$ , eq 1 should be sufficiently accurate.

To determine the integrated a → b absorption coefficient,  $\Gamma$ , we assume that the general spectral profile of the a → b band does not differ significantly from one solvent to the next. Indeed, for a variety of solvents, we have established that the a → b absorption band is modeled quite well by a Lorentzian profile.<sup>12</sup> Hence, the integrated absorption coefficient,  $\Gamma$ , in eq 1 can be expressed as a function of  $\epsilon_{\max}$  and  $\Delta\nu_{\text{fwhm}}$ .<sup>37</sup>

$$\Gamma = \frac{1}{2}\pi\epsilon_{\max}\Delta\nu_{\text{fwhm}} \quad (2)$$

To obtain a value of  $\Delta\nu_{\text{fwhm}}$  for the a → b transition in D<sub>2</sub>O that is arguably more accurate than what can be obtained from the data in Figure 2, we employ our observation that the bandwidths of a → b spectra correlate well with the bandwidths of a → X spectra.<sup>12</sup> On this basis, using the information provided by Dam et al.,<sup>12</sup> and given an a → X bandwidth in D<sub>2</sub>O of 108.3 cm<sup>-1</sup>,<sup>38</sup> we obtain a value of 75 ± 4 cm<sup>-1</sup> for the a → b  $\Delta\nu_{\text{fwhm}}$  in D<sub>2</sub>O.

Using eqs 1 and 2 and the data given in Table 1, we have calculated first-order radiative rate constants,  $k_{ba}$ , for the b → a transition in five solvents (Table 2). According to the dictates of Minaev's model, we then examine how these values of  $k_{ba}$  compare to the corresponding rate constants for the a → X transition by taking the ratio  $k_{aX}/k_{ba}$  (Table 2). In this regard, two points are worth noting. First, despite the large differences in these solvents and large differences in the respective values of  $k_{ba}$  and  $k_{aX}$ , we indeed find, as predicted, that the  $k_{aX}/k_{ba}$  ratio remains relatively constant. Second, our values of  $k_{aX}/k_{ba}$  are, on average, a factor of 2.5 times larger than that predicted by Minaev (∼3 × 10<sup>-4</sup>).<sup>18</sup> One should exercise restraint, however, when considering this latter point because (1) our values of  $k_{ba}$ ,

in the least, contain a systematic error associated with the use of eq 1 for such a weak, nominally forbidden transition (vide supra), (2) absolute values of  $k_{aX}$  are known with an accuracy of ∼±35% (Table 2), and (3) the accuracy of Minaev's prediction, although unspecified, likewise has its limitations.

In early work on the a → X transition, we established that the solvent-dependent, first-order radiative rate constant,  $k_{aX}$ , correlates reasonably well with the solvent refractive index,  $n$ , or functions of the refractive index [e.g.,  $(n^2 - 1)/(n^2 + 2)$ ].<sup>13,14,39</sup> Specifically,  $k_{aX}$  increases with an increase in  $n$ . The data thus indicate that the electronic response of the solvent (i.e., the optical polarizability) is a key parameter that must be considered in models that account for the perturbation of oxygen by the solvent. Schmidt and co-workers<sup>19,20</sup> have correspondingly shown that second-order a → X radiative rate constants, obtained by dividing the first-order rate constant by the concentration of the pertinent solvent, likewise correlate with the molar refraction of the solvent,  $R$ , obtained upon division of the function  $(n^2 - 1)/(n^2 + 2)$  by the solvent concentration. However, in their analysis of the second-order rate constants, Schmidt et al.<sup>19,20</sup> also considered the effect of the size of the perturbing solvent molecule as well as the oxygen-solvent collision frequency. Specifically, a size correction function was established by assuming that a given solvent molecule was a sphere of uniform polarizability. To this end, a correction factor of  $g(V_{\text{vdW}}) = V_{\text{vdW}}^{-2/3}$  was proposed, where  $V_{\text{vdW}}$  is the van der Waals volume of a given solvent molecule. It was likewise assumed that the oxygen-solvent collision frequency could be expressed by

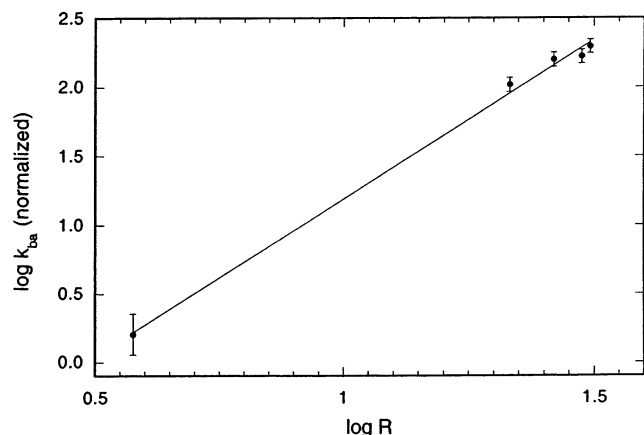
$$Z = d_{oc}^2 N_A \sqrt{\frac{8\pi kT}{\mu}} \quad (3)$$

where  $d_{oc}$  is the oxygen-solvent collision distance,  $\mu$  is the reduced mass of the colliding pair, and  $kT$  is the product of the Boltzmann constant and the absolute temperature. The collision distance  $d_{oc}$  is expressed in terms of oxygen and solvent parameters, respectively [ $d_{oc} = (d_o + d_c)/2$ , where  $d_o = 3.45$  Å and  $d_c = (6V_{\text{vdW}}/\pi N_A)^{1/3}$ ].

Upon dividing values of  $k_{aX}$  by the product  $g(V_{\text{vdW}})Zn^2$ , where  $n^2$  accounts for the expected dependence of the radiative rate constant on the solvent refractive index (eq 1), Hild and

**TABLE 3: Solvent Parameters Used To Obtain Normalized Values of  $k_{ba}$** 

solvent	$V_{vdw}^a$ (mL mol <sup>-1</sup> )	$d_c$ (Å)	$d_{oc}$ (Å)	$\mu$ (g mol <sup>-1</sup> )
D <sub>2</sub> O	11.5	3.32	3.39	12.3
CS <sub>2</sub>	31.2	4.63	4.04	22.5
benzene	48.4	5.36	4.41	22.7
<i>n</i> -hexane	68.3	6.01	4.73	23.3
toluene	59.5	5.74	4.60	23.8

<sup>a</sup> From Hild and Schmidt.<sup>20</sup>

**Figure 4.** Double logarithmic plot of the second-order radiative rate constant for the  $b \rightarrow a$  transition, normalized according to the method of Hild and Schmidt,<sup>20</sup> against the molar refraction of the solvent,  $R$  (mL mol<sup>-1</sup>). The solid line is a linear least-squares fit to the data and has a slope of  $2.3 \pm 0.3$ . The error on this value was determined using the slopes of the steepest and shallowest lines that could be drawn through the data using the given error bars.

Schmidt<sup>20</sup> demonstrated that the resultant normalized values of  $k_{aX}$  correlate well with the molar refraction,  $R$ , of the respective solvents. Specifically, upon plotting  $\log k_{aX}(\text{normalized})$  against  $\log R$ , a good linear correlation was observed. Moreover, a slope of 2 was obtained from this plot. This latter point indicates that the radiative rate constant  $k_{aX}$  is proportional to the square of the molar refraction  $R$ . In turn, because a radiative rate constant is likewise proportional to the square of the transition moment, the data appear to indicate that the solvent-induced transition dipole in oxygen indeed directly correlates with the solvent molar refraction and, hence, the electronic polarizability of a given solvent molecule.

Using solvent parameters listed in Table 3, we have likewise normalized our solution-phase values of  $k_{ba}$  according to the method of Hild and Schmidt.<sup>20</sup> The resultant, relative values of  $k_{ba}(\text{normalized})$  are shown in Table 2. Although we are dealing with a data set of limited size and although the D<sub>2</sub>O data are “remote” with respect to the data from the other solvents (hence emphasizing the importance of the present D<sub>2</sub>O study), we nevertheless find a reasonable correlation between  $k_{ba}(\text{normalized})$  and the solvent molar refraction. Moreover, in a plot of  $\log k_{ba}(\text{normalized})$  against  $\log R$  (Figure 4), we obtain a slope of  $2.3 \pm 0.3$ . In light of the data on the  $a \rightarrow X$  transition in which the analogous plot of  $\log k_{aX}$  against  $\log R$  had a slope of 2 (vide supra), the data shown in Figure 4 certainly give credence to Minaev’s model.

## Conclusions

Singlet oxygen, O<sub>2</sub>(<sup>1</sup>Δ<sub>g</sub>), dissolved in D<sub>2</sub>O, has been detected in a time-resolved near-IR absorption experiment. To extract this  $a \rightarrow b$  signal at  $\sim 5228$  cm<sup>-1</sup>, it was necessary to account for a laser-induced, temperature-dependent shift in a D<sub>2</sub>O

absorption band. The  $a \rightarrow b$  absorption coefficient obtained from these D<sub>2</sub>O data, along with  $a \rightarrow b$  data obtained in other solvents, give rise to solution-phase values of the  $b \rightarrow a$  radiative rate constant that cover a large range. In conjunction with complementary solution-phase data on the  $a \rightarrow X$  transition, the data reported herein give credence to a model proposed by Minaev<sup>16–18</sup> to account for the mechanism by which solvent induces transitions in oxygen.

**Acknowledgment.** This work was supported by a grant from the Danish Natural Science Research Council.

## References and Notes

- (1) Foote, C. S.; Clennan, E. L. In *Active Oxygen in Chemistry*; Foote, C. S., Valentine, J. S., Greenberg, A., Liebman, J. F., Eds.; Chapman and Hall: London, 1995; pp 105–140.
- (2) Scurlock, R. D.; Wang, B.; Ogilby, P. R.; Sheats, J. R.; Clough, R. L. *J. Am. Chem. Soc.* **1995**, *117*, 10194–10202.
- (3) Dougherty, T. J.; Gomer, C. J.; Henderson, B. W.; Jori, G.; Kessel, D.; Korbelik, M.; Moan, J.; Peng, Q. *J. Natl. Cancer Inst.* **1998**, *90*, 889–905.
- (4) Ogilby, P. R. *Acc. Chem. Res.* **1999**, *32*, 512–519.
- (5) Gorman, A. A.; Rodgers, M. A. J. In *Handbook of Organic Photochemistry*; Scaiano, J. C., Ed.; CRC Press: Boca Raton, FL, 1989; Vol. 2, pp 229–247.
- (6) Weldon, D.; Poulsen, T. D.; Mikkelsen, K. V.; Ogilby, P. R. *Photochem. Photobiol.* **1999**, *70*, 369–379.
- (7) Wilkinson, F.; Helman, W. P.; Ross, A. B. *J. Phys. Chem. Ref. Data* **1993**, *22*, 113–262.
- (8) Wilkinson, F.; Helman, W. P.; Ross, A. B. *J. Phys. Chem. Ref. Data* **1995**, *24*, 663–1021.
- (9) Weldon, D.; Ogilby, P. R. *J. Am. Chem. Soc.* **1998**, *120*, 12978–12979.
- (10) Keszthelyi, T.; Weldon, D.; Andersen, T. N.; Poulsen, T. D.; Mikkelsen, K. V.; Ogilby, P. R. *Photochem. Photobiol.* **1999**, *70*, 531–539.
- (11) Keszthelyi, T.; Poulsen, T. D.; Ogilby, P. R.; Mikkelsen, K. V. *J. Phys. Chem. A* **2000**, *104*, 10550–10555.
- (12) Dam, N.; Keszthelyi, T.; Andersen, L. K.; Mikkelsen, K. V.; Ogilby, P. R. *J. Phys. Chem. A* **2002**, *106*, 5263–5270.
- (13) Scurlock, R. D.; Ogilby, P. R. *J. Phys. Chem.* **1987**, *91*, 4599–4602.
- (14) Scurlock, R. D.; Nonell, S.; Braslavsky, S. E.; Ogilby, P. R. *J. Phys. Chem.* **1995**, *99*, 3521–3526.
- (15) Schmidt, R.; Afshari, E. *J. Phys. Chem.* **1990**, *94*, 4377–4378.
- (16) Minaev, B. F. *J. Mol. Struct. (THEOCHEM.)* **1989**, *183*, 207–214.
- (17) Minaev, B. F.; Lunell, S.; Kobzev, G. I. *J. Mol. Struct. (THEOCHEM.)* **1993**, *284*, 1–9.
- (18) Minaev, B. F.; Ågren, H. *J. Chem. Soc., Faraday Trans.* **1997**, *93*, 2231–2239.
- (19) Schmidt, R.; Bodesheim, M. *J. Phys. Chem.* **1995**, *99*, 15919–15924.
- (20) Hild, M.; Schmidt, R. *J. Phys. Chem. A* **1999**, *103*, 6091–6096.
- (21) Schmidt, R.; Bodesheim, M. *J. Phys. Chem. A* **1998**, *102*, 4769–4774.
- (22) *IUPAC Solubility Data Series. Volume 7: Oxygen and Ozone*; Battino, R., Ed.; Pergamon Press: Oxford, U.K., 1981.
- (23) Rodgers, M. A. J.; Snowden, P. T. *J. Am. Chem. Soc.* **1982**, *104*, 5541–5543.
- (24) Andersen, L. K.; Ogilby, P. R. *Rev. Sci. Instrum.*, in press.
- (25) Nonell, S.; Gonzalez, M.; Trull, F. R. *Afinidad* **1993**, *448*, 445–450.
- (26) Max, J.-J.; Chapados, C. *J. Chem. Phys.* **2002**, *116*, 4626–4642.
- (27) Deak, J. C.; Rhea, S. T.; Iwaki, L. K.; Dlott, D. D. *J. Phys. Chem. A* **2000**, *104*, 4866–4875.
- (28) Ogilby, P. R.; Foote, C. S. *J. Am. Chem. Soc.* **1982**, *104*, 2069–2070.
- (29) Libnau, F. O.; Toft, J.; Christy, A. A.; Kvalheim, O. M. *J. Am. Chem. Soc.* **1994**, *116*, 8311–8316.
- (30) Sasic, S.; Segtnan, V. H.; Ozaki, Y. *J. Phys. Chem. A* **2002**, *106*, 760–766.
- (31) Rödig, C.; Siebert, F. *Appl. Spectrosc.* **1999**, *53*, 893–901.
- (32) Braslavsky, S. E.; Heibel, G. E. *Chem. Rev.* **1992**, *92*, 1381–1410.
- (33) Rossbroich, G.; Garcia, N. A.; Braslavsky, S. E. *J. Photochem.* **1985**, *31*, 37–47.
- (34) Marti, C.; Jürgens, O.; Cuenca, O.; Casals, M.; Nonell, S. *J. Photochem. Photobiol., A. Chem.* **1996**, *97*, 11–18.
- (35) Strickler, S. J.; Berg, R. A. *J. Chem. Phys.* **1962**, *37*, 814–822.

(36) Poulsen, T. D.; Ogilby, P. R.; Mikkelsen, K. V. *J. Chem. Phys.* **1999**, *111*, 2678–2685.

(37) Gilbert, A.; Baggott, J. *Essentials of Molecular Photochemistry*; CRC Press: Boca Raton, FL, 1991.

(38) Wessels, J. M.; Rodgers, M. A. J. *J. Phys. Chem.* **1995**, *99*, 17586–17592.

(39) Poulsen, T. D.; Ogilby, P. R.; Mikkelsen, K. V. *J. Phys. Chem. A* **1998**, *102*, 9829–9832.